ACS APPLIED MATERIALS & INTERFACES

RESEARCH ARTICLE

www.acsami.org

Ordered Carbon Nanotubes for Optical Power Limiting Devices

Liran Katz,[†,‡] Ariela Donval,[§] Eyal Zussman,[†] and Yachin Cohen*[,‡]

[†]Department of Chemical Engineering and [‡]Mechanical Engineering, Technion-Israel Institute of Technology, Haifa, Israel 32000

[§]KiloLambda Technologies, Ltd., Tel-Aviv, Israel 69719

Supporting Information

ABSTRACT: The electrospinning (ES) process was used to fabricate composite nanofibers (NFs) of poly(methyl methacrylate), PMMA, with embedded multiwalled carbon nanotubes (MWNTs) from a solution of PMMA in N,N-dimethylformamide (DMF) with homogenously dispersed MWNTs. Using both the sinklike and the elongation flows in the electrospinning process, we aligned the carbon nanotubes (CNTs) along the fiber axis. The NFs were subsequently deposited in an aligned manner on a glass surface using the electrostatic lens created by the edge of a rotating wheel collector. Semitransparent optical power limiter (OPL) films (~50% transmittance) were fabricated using an optically compatible polymeric resin infiltrated into the collected NFs. These comprised oriented NFs with different carbon nanotube loadings and film thicknesses. The OPLs exhibited high limiting abilities, with a limiting threshold of 1.5 J/cm^2 at about 50% linear transmittance. Some degree of polarization was also achieved, but significantly lower than expected because of the NF orientation.

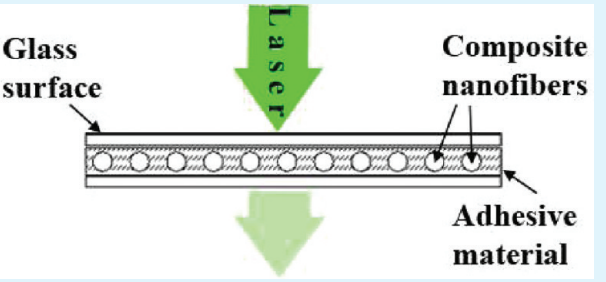

KEYWORDS: optical power limiting, carbon nanotubes, electrospinning, nanofibers, films, dispersion, polarization

INTRODUCTION

Optical power limiting (OPL) components made of artificial nanostructured materials are highly desirable for the protection of various optical instruments, from fiber-optic telecommunication systems to everyday life purposes, such as sunglasses and windows. The ability to control and regulate high intensities of light using only nonlinear light-matter interactions make OPL components simple and low-cost substitutes compared to conventional external (e.g., mechanical or electrical) options. Whereas a standard source of light behaves in a proportional-linear manner interacting with a material, a high-intensity light source, such as a laser, creates a polarization response with matter that is nonlinear in character.[1] The nonlinear interactions generated between the light and the medium can be exploited by optical modulators, such as optical power control devices.[2−6] One of the applications for light modulating is optical limiters,[3] which can limit high intensity light while allowing high transmittance of low intensity ambient light. Carbon nanotubes (CNTs), among other organic materials, were shown to have strong nonlinear effects in addition to their unique electrical and mechanical characteristics.[7−18] Whereas carbon black suspensions (CBS) possess broadband optical limiting and fullerenes have diverse functionality to different materials, CNTs consist of both of the aforementioned attributes. Chen and co-workers[16] were the first to report about the optical limiting properties of CNT's. They revealed a superior limiting behavior of the CNTs compared to CBS and fullerenes, although they were in a suspension form. CNT suspensions can be stable but not for long, and additionally can generate heterogonous aggregates, which can affect the uniformity of the limiting effect. Therefore, much effort has been made to transform the suspensions into stable CNT solutions using different methods, such as coating, doping and blending with optical absorbing dye.[17] Qiu et al.[15] grafted polymers such as PMMA to the surface of the multiwalled carbon nanotubes (MWNTs) in solution and showed better limiting performance than those of pristine MWNTs and C_{60}. So far, the majority of research has been concentrated on CNT dispersions and suspensions although they are not applicable for practical application. There have been only few reports on the limiting properties of CNTs in a solid matrix. Solid state limiters, such as CNTs embedded into polymer films, can bring higher stability in long-range usage. Sun et al.[8] examined the limiting properties of embedded MWNTs in poly(methyl methacrylate), PMMA, film and compared them with MWNTs suspended in water. This study showed that the limiting threshold (i.e., the input fluence at which the transmittance falls to 50% of the linear transmittance) of the films were higher (therefore, worse) than the suspension (at 532 nm). Although the films showed inferior limiting properties compared to the suspension, further development is needed to reach a better limiting performance.

Because of their elongated tubular structures made of graphite layers, CNTs exhibit strong optical absorption. The $\pi-\pi^*$ electrons' transition and the plasma frequency of graphite π electrons (i.e., ~7 eV) are the reasons for the strong optical absorption in the visible region, as well as in the ultraviolet and infrared regions.[19] Light waves traveling in a parallel orientation

Received: August 1, 2011
Accepted: November 5, 2011
Published: November 06, 2011

ACS Publications © 2011 American Chemical Society

Table 1. Experimental Parameters of Electrospun Film Fabrication

	random fiber mat	oriented fiber mats		
	Set1	Set2	Set3	Set4
PMMA content in solution (wt %)	10.0	10.0	10.0	8.5
MWNTs in PMMA (wt %)	2.5		2.5	2.5
MSM/MWNT ratio (w/w)	2/1		2/1	2/1
working distance (cm)	9.5	9.0	9.5	9.5
tangential velocity (m/s)	0.5	12	20	20
high voltage (kV)	15.5	12.5	16.0	17.5
type of collector[a]	H	V	V	V
needle diameter (gauge)	25G	25G	25G	25G
solution flow rate (mL/h)	1.2	0.8	1.2	1.2
collecting time (min)	45, 60, 90	15, 30, 45	30, 45, 90, 120	30, 60, 90, 120

[a] H, horizontal; V, vertical.

to the aligned CNTs are absorbed, whereas light waves in perpendicular or diagonal orientations to the CNTs are refracted or transmitted between the vacancies of the aligned nanotubes, NTs.[19,20] Therefore, aligned anisotropic CNTs in a solution or film can be used as a polarizer in addition to their limiting abilities. Bubke and co-workers[21] examined the optical effects caused by an electric field on CNT solution. A high state of polarization was clearly observed by changing the direction of the polarized light entering the dispersion. In a different work,[19] an optical polarizer film was fabricated of single-walled carbon nanotubes (SWNTs) in poly(vinyl alcohol)- PVA on a glass plate. Using mechanical stretching of the film and short CNTs (mean length of 200 nm), degree of polarization (DOP) and unpolarized transmission were 86.6 and 12.0%, respectively.

One way to achieve homogeneously dispersed and aligned CNTs in a polymeric matrix is by using the electrospinning (ES) technique, a low-cost and simple method to create fibers in the nano- to micrometer-scale range.[22,23] When high voltage is applied to the tip of the syringe needle (up to 30 kV), the pendant drop of the material solution will become highly electrified and induced surface charges will appear. As a result of electrostatic forces the shape of the drop will be distorted to a conical shape also known as a Taylor cone.[24] When the electric field power transcends a certain threshold (i.e., overcoming the surface tension of the solution), a liquid jet will be formed creating a sinklike flow having the ability to align the CNTs inside the formed fiber. During the uniaxial stretching of the jet by bending instabilities, evaporation of the solvent takes place creating a solidified fiber.[25] In addition to the intrinsic alignment of CNTs, fiber alignment can be done by various collecting methods such as, rotating disk,[26,27] patterned electrodes,[28,29] two magnets with a gap,[30,31] etc.[32] Extensive research has been done on the embedment of CNTs into electrospun fibers.[33−37] However, the small number of articles concerning CNT-based optical limiters and polarizers gives rise to the need for more investigations and development in this area.

On the basis of previous achievements and developments, we utilized the intrinsic and structural properties of the CNTs to fabricate a composite film made of electrospun PMMA nanofibers (NFs) embedded with MWNTs for the creation of optical power limiter and polarizer. In this paper, we report the experimenting of different solvents and their effect on the PMMA fiber's morphology. High oriented films with different thicknesses and MWNT compositions are measured for their linear transmittance, nonlinear response, and polarization.

Table 2. Experimental Parameters of Optical Device Fabrication

ES parameters (Table 1)[a]	device notation[b]	ES collecting time (min)	resin type
Set1	D1-T45	45	AB9075
	D2-T60	60	
	D3-T90	90	
Set2	Control-1	45	AB9075
	Control-2	45	OP-30
Set3	D4-T30	30	AB9075
	D5-T45	45	
	D6-T90	90	
	D7-T120	120	
	D8-T30	30	OP-30
	D9-T45	45	
	D10-T90	90	
	D11-T120	120	
Set4	D12-T60	60	AB9075
	D13-T90	90	
	D14-T120	120	
Control	Control-3		AB9075
	Control-4		OP-30

[a] The different sets are referred to the experimental parameters presented in Table 1. [b] D# denotes device number and T# denotes the collection time (min).

MATERIALS AND METHODS

Pristine MWNTs were procured from Arry International (Cologne, Germany) with a diameter of 20−30 nm and length of 0.5−2 μm (purity >95 wt %) and were used without additional purification or modification procedures. N,N-dimethylformamide (DMF) was purchased from Frutarom (Israel) and used as-received. The triblock copolymer poly(methyl methacrylate-b-styrene-b-methyl methacrylate) − MSM with $\overline{M}_n$ of ~230 000-b-162 000-b-230 000 g/mol was purchased from Polymer Source (Montreal, Canada). It served as surfactant for dispersing MWNTs in solution and was used as-received. The polymer matrix material, PMMA of $\overline{M}_w$ ~350 000 g/mol, was acquired from Sigma

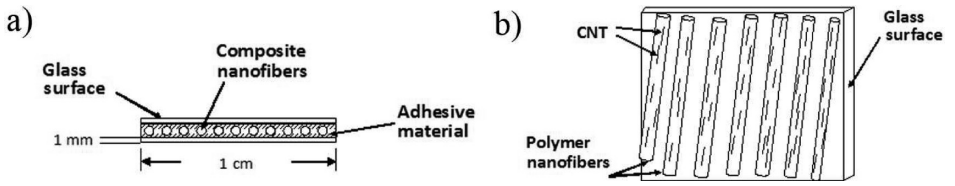

Figure 1. Scheme of an OPL device; (a) Side and (b) Upper view.

Aldrich and was used as-received. UV/visible cure optical resins (Dymax OP-30, AngstromBond AB9075) were used to seal the film in between two glass slides.

Dispersion of MWNTs in DMF/PMMA Solutions. MWNTs and MSM were added to the DMF solvent in different concentrations and were ultrasonicated using a tip sonicator (VCX750, frequency 60 Hz, power 750 W, Vibracell Inc.) for 8 min at 50 W followed by mild sonication using a bath sonicator (DC150H, frequency 40 kHz, MRC Inc.) for 90 min to create initial black-colored dispersions. PMMA was then added and mechanically stirred overnight at 70 °C using a magnetic stirrer to create homogeneous mixtures. The mixtures were then centrifuged (at 4500 rpm and in time range of 15−25 min) and the supernatants, which were decanted from the mixtures, were bath-sonicated for 6 h (1.5 h sonication intervals followed by 30 min pause to cool the system and the mixtures) and then used for the remainder of the process.

Fabrication and Collection of Composite NFs. The ES technique was used to fabricate PMMA NFs and PMMA/MWNTs NFs. A positive high voltage generated by a high voltage power supply (FC40P3, power 120 W, Glassman Inc.) was applied to the solution via copper wire. The solution was inserted into a plastic syringe with a stainless steel needle of varying diameter. The rate of solution flow out of the needle was controlled by a syringe pump (Harvard Apparatus Inc.). Grounded conductive collectors were used at different working distances from the syringe. For each solution composition, the ES conditions were varied accordingly to obtain a stable jet (as presented in Table 1 for four cases). All ES processes were conducted at ambient temperature while two systems of grounded collectors were used for the different cases. The collecting substrate for the application was a glass plate (dimensions 2.6 × 1.0 × 0.1 cm^3) that was attached to the collectors in order to collect oriented and random films of NFs using a vertical rotating wheel and a horizontal rotating wheel, respectively. The duration of fiber collection was varied in order to obtain different film thicknesses.

Construction of the Optical Device. Sealing of the device was made by a glass cover slide similar in composition and dimensions to the collecting slide, which was glued to the exposed surface of the film using UV/visible cure optical resins. The resins used for gluing were then cured using a UV curing spot lamp (BlueWave 200, Dymax Inc.) for several minutes at 19 mW/cm^2. Table 2 and Figure 1 present the parameters of different fabricated devices discussed below and a scheme of the OPL device, respectively.

Characterization. The initial morphological parameters of the as-spun NFs (e.g., approximate diameter, presence of beads and drops) were observed using light optical microscope (LOM) (BX15, Olympus Inc.) and recorded using CCD camera (DP12, Olympus Inc.). Desktop scanning electron microscope (SEM) (G2, Phenom-World Inc.) was used to determine cross section of the film, orientation of NFs in the upper layers of the film and final morphological parameters, at an acceleration voltage of 5 kV. For the cross-section imaging, the film was clean cut perpendicularly to the fibers' direction using an industrial blade under liquid nitrogen. A close inspection of the fiber's surface morphology generated from solutions with different solvents was obtained using high resolution (HR)-SEM (Ultra Plus, Zeiss Inc.). The images were taken using SE2 and InLens detectors at an acceleration voltage of 1 kV and a working distance of 2.5−3.5 mm. The presence of MWNTs in PMMA NFs was characterized using TEM (Tecnai T12 G^2, FEI Inc.) at an acceleration voltage of 120 kV. The images were captured using a US1000 high-resolution CCD camera. The linear transmittance of visible light through the fabricated optical device was examined by an optic fiber spectrometer system composed of Visible-near IR light source (H-2000, Avantes Inc.) and fiber-optic spectrometer (Avantes Inc.). The transmittance was measured at wavelengths of 400−700 nm and the light source beam diameter was 1−2 mm. The limiting properties of the device were studied using a nonlinear response laser system. The system was composed of a Q-switched Nd:YAG nanosecond single pulse laser (Blue Sky Inc.) operating at 532 nm, input energy detector, f/5 focusing geometry (including aperture and input lens), mounted experimental device, f/6 focusing geometry (including aperture and output lens), and output energy detector. The input energy varies from 0.1 μJ and up to 100 μJ. The device was positioned in the focal point of the laser beam and the output energy was measured as a function of the input energy. The polarizing abilities of the device were examined by an experimental setup as follows: the incident laser beam generated from a solid state laser operating continuously at 532 nm (50 mW, BWTEK Inc.) was linearly polarized by a polarizer at angle α. The intensity of light passing through the polarizer/sample setup with the sample director either parallel or perpendicular to the polarizer direction was measured. A second polarizer set in a direction parallel to the first one was placed before the detector in order to minimize noise.

RESULTS AND DISCUSSION

Film Fabrication of Electrospun PMMA/MWNTs NFs. PMMA and PMMA/MWNTs NFs were fabricated using the ES process to form different sets of fibers (see Table 1 for experimental parameters): Set1 comprised a thick (mean diameter of 720 nm) random mat of PMMA/MWNTs NFs, Set2 comprised an oriented mat of PMMA NFs, Set3 and Set4 were comprised of oriented mats of thick (mean diameter of 720 nm) and thin (mean diameter of 460 nm) PMMA/MWNTs NFs, respectively.

When fibers solidify after evaporation of the solvent, "defects" on their surface, such as pits or crates, can appear and cause unwanted interactions of incident light with the fibers. Early trials of different solvents showed differences in morphology between the as-spun PMMA NFs, as can be seen in the HR-SEM images of Figure 2. Therefore, the choice of solvent is one of the most important factors for the desired uniform fiber structure. Nitromethane was examined as a solvent in the PMMA system due to its high solubility parameters (δ_p = 18.8, δ_t = 25.1 [$MPa^{0.5}$]) compared to commonly used solvents for the dispersion of CNTs in polymer matrix of PMMA.[38] The fabricated NFs showed a porous morphology (Figure 2a). The formation of pores was caused by the high evaporation rate of the solvent during fiber formation. DMF/Acetone solvent mixture at different ratios combines a high dielectric constant

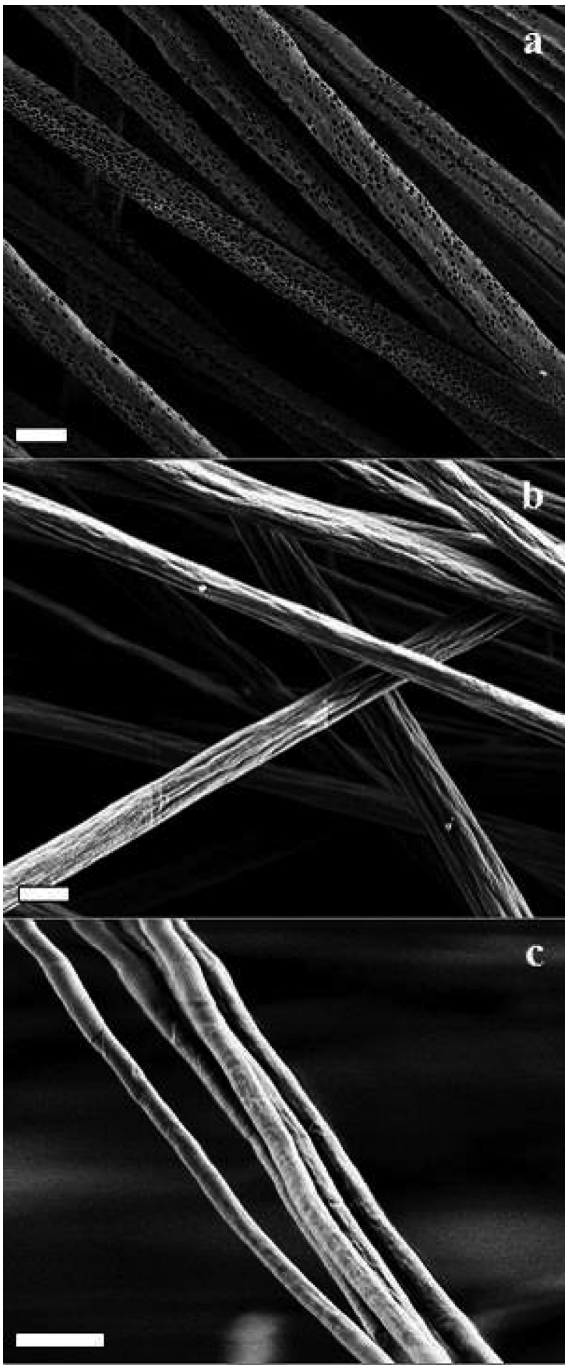

Figure 2. HR-SEM images of 10 wt % electrospun PMMA fibers in (a) nitromethane (b) DMF:acetone (40:60 w/w), (c) DMF. Scale bars = 2 μm.

and intermediate evaporation rate for the creation of electrospun fibers. A grooved morphology of the fibers was found when this mixture was used, as can be seen in Figure 2b. DMF showed good fiber morphology with smooth and uniform structure and was thus used solely for the entire process (Figure 2c).

Under the same ES conditions, PMMA/MWNTs NFs were fabricated as indicated in Table 1. LOM imaging (Figure 3) showed fibers without beads and fiber surface, which did not exhibit drops from solution residues at the end of the dispersion process.

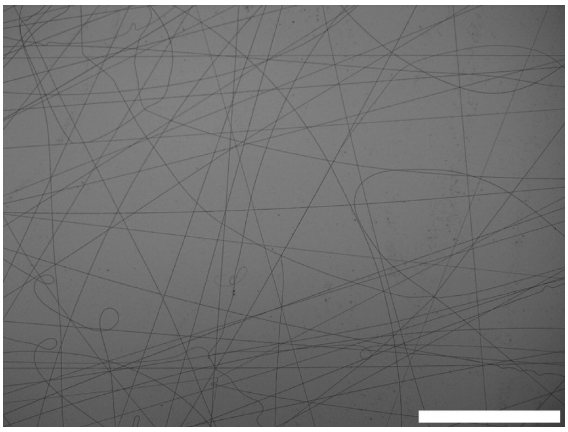

Figure 3. LOM image of PMMA/MWNTs as-spun NFs (Set3). The dispersion process was performed entirely. Scale bar = 500 μm.

TEM imaging clearly depicts the presence of MWNTs in the PMMA NFs, as can be seen in Figure 4. The NTs were generally aligned along the fiber's axis, whereas some segments of the nanotubes showed deviation from the desired direction. The NFs for TEM imaging were collected on a TEM grid held in the gap between the syringe and collector. Thus, the observed diameters of the fibers are not the typical diameter of a final fiber because of further uniaxial stretching up to the final collection.

The diameter of the NFs was changed in order to examine its effect on the optical performance of the fabricated device. For this purpose, the polymer concentration was reduced from 10 to 8.5 wt % PMMA in solution while other parameters remained constant. This led to reduction of about 40% in the fibers' diameter, as can be seen in Table 3. Two contributions can affect the reduction of fiber diameter: the change in solution concentration and the change in conductivity caused by the change in MWNTs concentration. It was shown experimentally and theoretically[39−41] that polymer concentration has a significant effect on the diameter of the fiber. It is known that viscosity has a power law relation with the polymer concentration as: $\eta \propto C^{\beta}$,[39] where C is the polymer concentration and β is a constant. If we consider that the electrospun fiber diameter increases with solution viscosity as $d \propto \eta^{\gamma}$, where d is the fiber diameter, η is the solution viscosity, and γ is a constant, then it is expected that $d \propto C^{\delta}$, where δ is the scaling exponent. For electrospun fibers from PMMA dissolved in DMF, δ was found experimentally to be 3.1.[40] This corresponds to ~40% change in the fiber diameter due to a decrease in concentration, as shown in Table 3. The second contribution to the change in the fiber diameter was most likely negligible due to the minor change in the MWNTs concentration, even though increased conductivity caused by the addition of MWNTs to the solution is a known phenomenon yielding thinner fibers.[34]

The use of a vertical rotating wheel (at rotation speeds of up to 2000 rpm and diameter of 20 cm) for the collection of fibers showed a high degree of fiber orientation. SEM imaging (Figure 5) shows one example of a film constructed from oriented fibers. From inspection of the image, the orientation of about 100 fibers was measured relative to the main director of the film (which was parallel to the long axis of the glass plate). It was found that the orientation distribution was such that one standard deviation from the main director was at an angle of about 14°.

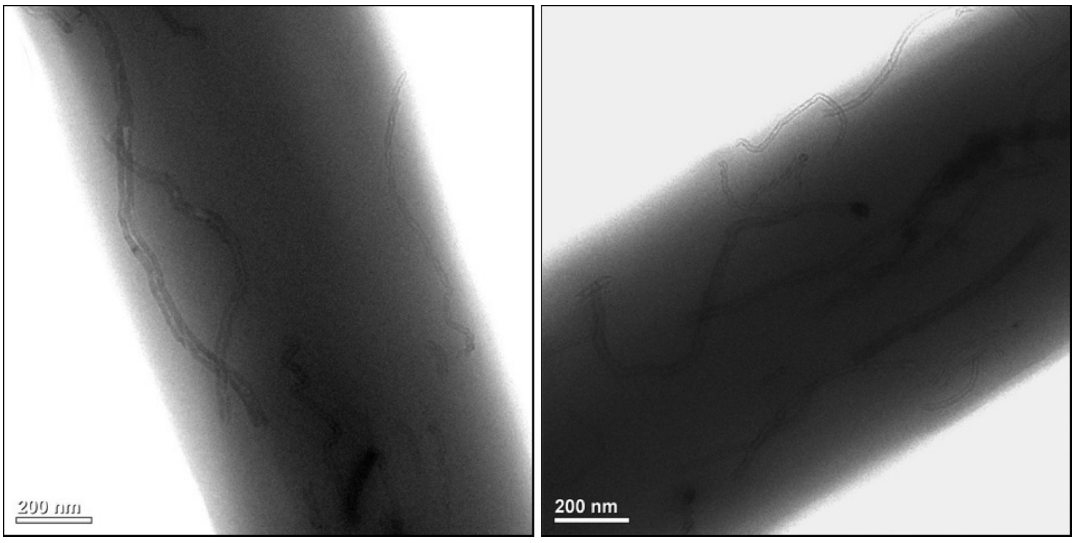

Figure 4. TEM images of PMMA/MWNTs electrospun NFs (Set4). Scale bars = 200 nm.

Table 3. Diameter Distribution and Size in Different Sets of Experiments

	PMMA/MWNTs NFs	
	Set3	Set4
average diameter (nm)	720 ± 48	460 ± 115

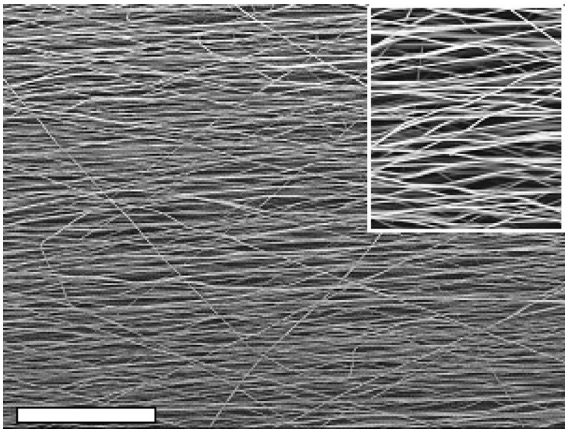

Figure 5. SEM image of PMMA/MWNTs film at 45 min collection time (Set3). Scale bar = 80 μm. Inset shows magnification of the image.

The thickness of the film was controlled by the collection time of the fibers onto the collector surface when other parameters (such as, solution flow rate, collection method and polymer concentration) remained constant for each set of experiments. For example, for films made of Set3 (0.25 wt % MWNTs and 10 wt % PMMA in the solution, surfactant/MWNTs ratio 2:1 w/w), a higher collection time exhibited a thicker film (Figure 6), although the behavior was not a linear one, as can be seen in Figure 7. A sharp rise in thickness occurred up to a certain value (collection time of 45 min). Above this value, a moderate rise was observed up to 90 min. This phenomenon occurred, apparently, because of a greater electrostatic repulsion between the fibers

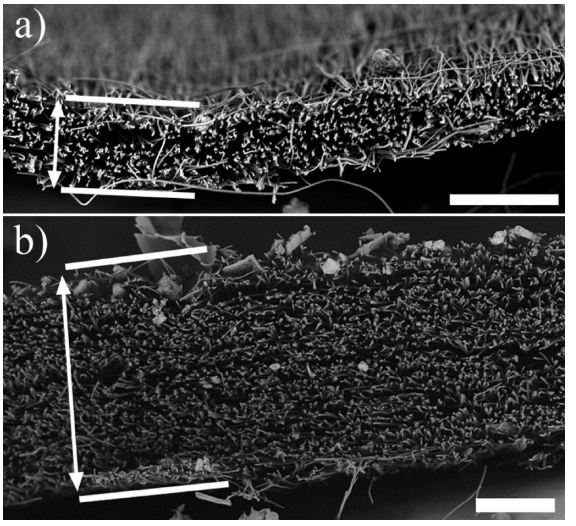

Figure 6. SEM images of PMMA/MWNTs film cross-section at (a) 30 min collection time and (b) 90 min collection time (Set3). Scale bars = 50 μm.

during their alignment and deposition on the collector's surface.[27] Therefore, at a certain thickness, the discharge time of the free surface electrons located on the deposited fibers became longer. The prolonged discharge time caused the subsequent fibers to be pushed to the collector's sides.

OPL Optical Characteristics. Optical devices were fabricated by spreading optical adhesive resin on the film and sealing it by a cover glass slide. Optical devices differ by collection times and two resin types as listed in Table 2.

For practical purpose relevant to the use of OPL devices, it is desirable to ensure low opacity as much as possible. Thus, a lower bound for the light transmittance of the optical devices was set in this work to be about 50%. The linear transmittance of visible light evaluated as a function of film thickness (collection time) is shown in Figure 8 for optical devices made using fabrication parameters of Set3 and the relevant control. The measurements were conducted using OP-30 and AB9075 optical adhesives after curing. The control samples were made of the resin alone and the

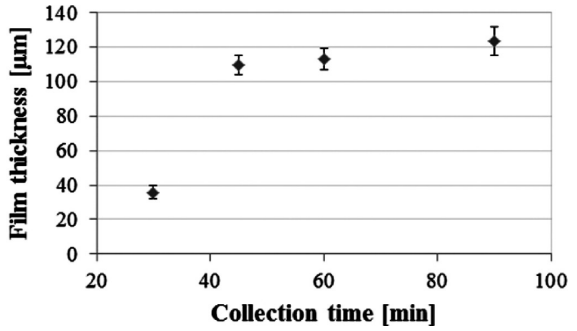

Figure 7. Film thickness as a function of collection time (Set3).

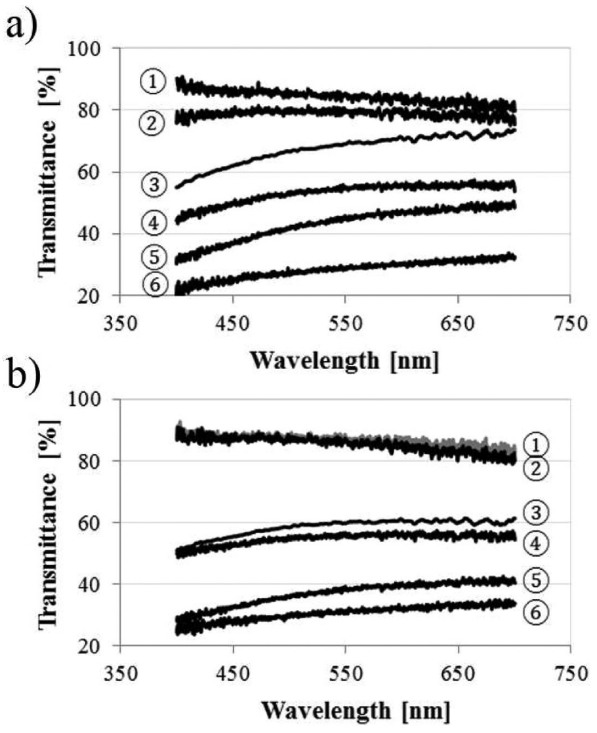

Figure 8. Linear transmittance as a function of wavelength in the visible light spectrum for films of different thickness (different collection times), Set3. (a) OP-30 resin: (1) Control-4, (2) Control-2; devices (3) D8-T30, (4) D9-T45, (5) D10-T90, and (6) D11-T120. (b) AB9075 resin: (1) Control-3, (2) Control-1; devices (3) D4-T30, (4) D5-T45, (5) D6-T90, and (6) D7-T120.

resin-impregnated PMMA NF films showed similar light transmittance with the AB9075 resin (Figure 8b) but a lower transmittance was observed with the NFs in the OP-30 (Figure 8a). These results indicate better optical compatibility of AB9075 with the NF material, as compared with OP-30, due to similarity in refractive index (RI) between AB9075 and PMMA (RI = 1.49 for both, whereas for OP-30, RI ≈ 1.51). In addition, an increase in film thickness caused a decrease in transmittance observed in all of the studied cases. A continuous behavior of light transmittance was observed for each one of the curves in the visible light region. AB9075 was used for further optical measurements because of its better optical compatibility.

The optical devices showed an evident nonlinear response as the MWNTs were embedded in the PMMA NFs. The data

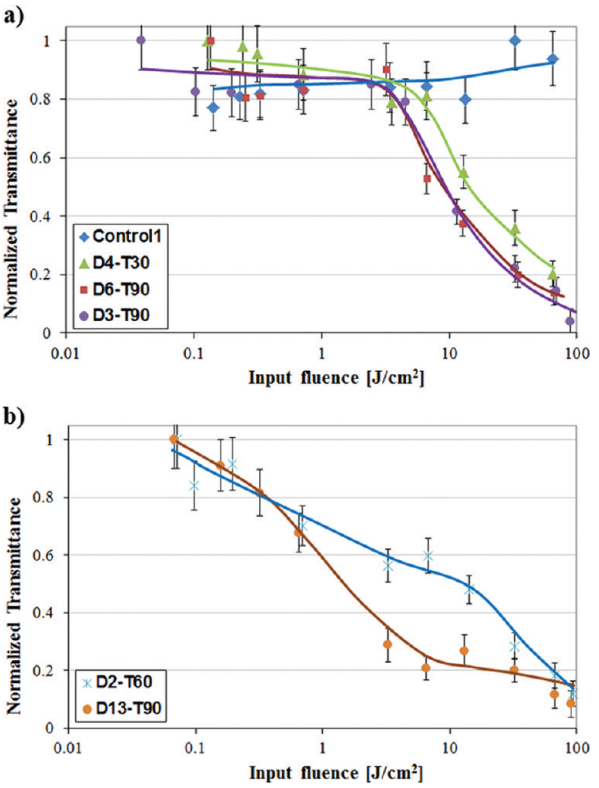

Figure 9. Normalized transmittance as a function of input fluence: (a) comparison of the control device (without CNTs) with two devices of similar makeup and different thickness (D4-T30, D6-T90) and devices with random and aligned NFs of the same makeup and thickness (D3-T90, D6-T90). (b) Two devices that differ by nearly an order of magnitude in their limiting threshold. The lines through the data points are intended only for visual guide.

provided in Figure 9a represent different sets of optical devices: a comparison of two devices of similar makeup and different thickness (collection time), and two devices with random and aligned NFs of the same makeup and thickness. It should be noted that the Control-1 sample is composed only of PMMA fibers and the cured AB9075 resin. For example, D6-T90 sample (Set3) showed linear response at low input fluences until it reached a certain threshold (input fluence ~3 J/cm^2). At input fluences higher than 3 J/cm^2, a nonlinear response occurred when the normalized transmittance (eq 1) was sharply decreased. Thicker films (longer collection time) exhibited a lower limiting threshold, as can be observed in Figure 9. Thus, a thicker layer of film containing a higher percentage of MWNTs enhanced the nonlinear phenomena and created a lower limiting threshold. Films with oriented and nonoriented fibers showed a similar nonlinear response, as can be seen by comparison of the response of D3-T90 and D6-T90 samples. The nonlinear optical response is sensitive to several parameters of the processing conditions, dispersion properties, etc. For example, Figure 9b presents the nonlinear response of two devices that differ by nearly an order of magnitude in their limiting threshold. These samples differ in the dispersion concentration, NFs alignment and thickness. The current results do not provide a direct indication for the source of enhanced OPL characteristics. However, the best results appear with thinner and aligned NFs. TEM observations indicate that CNTs align better in thinner NFs, so that the laser beam polarization interacting with

Table 4. Light Limiting Properties of the Examined Optical Devices and Their Normalization

set no.[a]	device no.	limiting threshold (input fluence) (J/cm^2)	normalized limiting threshold	linear transmittance (%)	quality factor
ref 8		3.1	1.0	50	2.0
Set3	D8-T30	17	5.5	68	8.1
	D10-T90	9	2.9	45	6.5
Set4	D12-T60	6	1.9	67	2.9
	D13-T90	1.5	0.5	48	1.0
Set1	D2-T60	15	4.8	48	10.0
	D3-T90	9	2.9	45	6.5

[a] The different sets are referred to the experimental parameters presented in Tables 2 and 3.

the CNT dipole moment is expected to lead to enhanced nonlinear effect. The transmittance depicted in figure 9 is normalized by eq 1

$$T_{\text{normalized}}(E_{\text{in}}) = \frac{E_{\text{out}}(E_{\text{in}})/E_{\text{in}}}{E_{\text{out}}(E_{\text{in}}{}^{*})/E_{\text{in}}{}^{*}} \quad (1)$$

where $E_{\text{out}}(E_{\text{in}})$ is the output energy as a function of the input energy E_{in}, $E_{\text{out}}(E_{\text{in}}{}^{*})$ is the output energy when the input energy is below the threshold of nonlinear behavior, and for which the highest transmittance is observed (which usually is the lowest input energy)

The nonlinear optical response and the observation of a limiting threshold are a major goal of this research. To compare the response of the different samples, we conducted two normalizations. The limiting threshold values (the fluence at which the transmittance falls to half its initial linear value) of all measured samples were normalized to a comparative value taken from the literature for MWNTs in PMMA film (3.1 J/cm^2).[8] Furthermore, to correct for the fact that those thicker samples with more CNTs may have a lower limiting threshold value at the cost of lower transmittance, the normalized limiting threshold was divided by the sample's linear transmittance. The factor thus calculated is set to be the "quality factor" (QF) for the limiting threshold effect. A desired value should be smaller than the QF of the best published data, a value of 2.0.[8] The results of the optical limiting measurements are presented in Table 4. It can be seen that sample D13-T90 made of oriented NFs containing CNT exhibited the best results with a normalized limiting threshold value of 0.5 at 48% linear transmission, and QF of about 1. This is better than reported in the literature so far for solid devices. From Table 4, it can also be seen that the oriented thinner fibers (Set4) exhibit enhanced performance as compared to the thicker ones (Set3).

Polarization is also a desirable property of OPL devices, which may be readily achieved by the ES process. The polarization properties of the device were compared between different sets of experiments: Nonoriented fibers (Set1), oriented fibers (Set3) and oriented thin fibers (Set4). Figure 10 shows the measured polarization values (DOP, eq 2) as a function of the sample transmittance (to account for optical density due to CNT content). The nonoriented fibers were shown to have very low DOP (<0.05). The two sets of oriented fibers showed much higher values of DOP (maximum DOP value of 0.31 at 31% transmittance). The thinning of the fibers did not seem to help

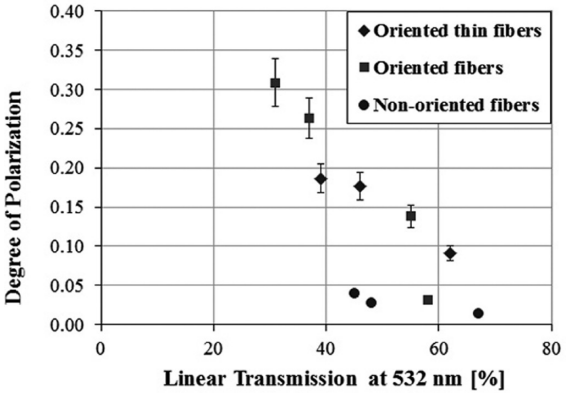

Figure 10. Degree of polarization as a function of linear transmission at different cases: Oriented thin fibers (Set4), oriented fibers (Set3), and random fibers (Set1).

achieve better DOP and in some cases even made it worse. Apparently CNT alignment within the NFs is hindered by their structural irregularities. Better selection of CNT raw material and more work need to be done in order to achieve better polarization. The calculation of the degree of polarization was made by the following equation[42]

$$\text{DOP} = \frac{E_{\text{max}} - E_{\text{min}}}{E_{\text{max}} + E_{\text{min}}} \quad (2)$$

where E_{max} is the maximum output energy (i.e., perpendicular position) and E_{min} is the minimum output energy (i.e., parallel position).

CONCLUSIONS

The work done in this research intended to create an optical device that would act as a light limiter and polarizer. The ability to use CNTs as optical modifiers was examined in this work by incorporating them into polymer matrices using the ES process. PMMA/MWNT NFs with a smooth and uniform morphology were successfully fabricated using the ES process. The uniform distribution and general longitudinal alignment of the MWNTs in the fiber was noticeable and was mainly attributed to the quality of the solution dispersion and to the elongation forces generated by the ES jet flow. The use of a rotating wheel as the collector enabled a high degree of fiber orientation in the as-produced films.

The NFs in the spun films were embedded in an optical-grade resin with compatible refractive resin thus creating optical devices with uniform optical properties and excellent optical limiting behavior, better than reported in the literature for solid-state optical limiters. Thinning the NFs resulted in enhanced limiting performance. On the other hand, the poor alignment of MWNTs in the fiber resulted in low polarization. Although the tubes' general alignment and their uniform dispersion in the fiber were observed, some segmental parts of the tubes appear twisted and contorted, which is deleterious for the desired polarization. One way to achieve better MWNT alignment in the fiber is to enhance the elongation flow by narrowing the diameter of ES jet and hence the as-spun NFs. Furthermore, the use of different CNT sources having shorter and/or straighter shape of the tubes may be useful. Polymer matrices other than PMMA may also be considered.

■ ASSOCIATED CONTENT

Supporting Information. Scheme of the ES process setup, and schemes of the optical nonlinear response and polarizing systems (PDF). This material is available free of charge via the Internet at http://pubs.acs.org.

■ AUTHOR INFORMATION

Corresponding Author
*E-mail: yachinc@tx.technion.ac.il.

■ ACKNOWLEDGMENT

L.K. acknowledges a partial support from the Leonard and Diane Sherman Interdisciplinary Graduate School Fellowships. Financial support from the NES MAGNET project of the Israel Ministry of Trade and Industry is gratefully acknowledged. We thank the help of Mrs. Naama Koifman and Dr. Judith Schmidt on TEM and HR-SEM.

■ REFERENCES

(1) Boyd, R. W.; Masters, B. R. *Nonlinear Optics*, 2nd ed.; Academic Press: New York, 2003.
(2) Choudhury, A. N. M. M.; Grzegorzewska, B.; Hanrahan, T.; Marrapode, T.; Donval, A.; Oron, M.; Oron, R.; Shvartzer, R. *National Fiber Optic Engineers Conference*; March 25−29, 2007; IEEE: Piscataway, NJ, 2007; JThA88
(3) Donval, A.; Fisher, T.; Nemet, B.; Oron, R.; Oron, M.; Shvartzer, R.; Eberle, B.; Ritt, G.; Ebert, R. *Infrared Technology and Applications XXXIV*; Orlando, FL, March 16−20, 2008; SPIE: Bellingham, WA, 2008; Vol. 6940, 69400Z−69400Z-10.
(4) Donval, A.; Nemet, B.; Oron, M.; Oron, R.; Shvartzer, R. *Technical Proceedings of the 2007 NSTI Nanotechnology Conference and Trade Show*; Nano Science and Technology Institute: Austin, TX, 2007; Vol. 1, pp 100−103.
(5) Donval, A.; Nemet, B.; Shvartzer, R.; Oron, M. *Technical Proceedings of the 2008 NSTI Nanotechnology Conference and Trade Show*; Nano Science and Technology Institute: Austin, TX, 2008; Vol. 3, pp 17−21.
(6) Donval, A.; Goldstein, S.; McIlroy, P.; Oron, R.; Oron, M. B.; Patlakh, A. *Proc. SPIE* **2004**, *5577*, 724–728.
(7) Riggs, J. E.; Walker, D. B.; Carroll, D. L.; Sun, Y. *J. Phys. Chem. B* **2000**, *104*, 7071–7076.
(8) Sun, X.; Yu, R. Q.; Xu, G. Q.; Hor, T. S. A.; Ji, W. *Appl. Phys. Lett.* **1998**, *73*, 3632–3634.
(9) Vivien, L.; Anglaret, E.; Riehl, D.; Hache, F.; Bacou, F.; Andrieux, M.; Lafonta, F.; Journet, C.; Goze, C.; Brunet, M.; Bernier, P. *Opt. Commun.* **2000**, *174*, 271–275.
(10) Vivien, L.; Lançon, P.; Riehl, D.; Hache, F.; Anglaret, E. *Carbon* **2002**, *40*, 1789–1797.
(11) Wang, J.; Blau, W. J. *Appl. Phys. B: Lasers Opt.* **2008**, *91*, 521–524.
(12) Wang, J.; Chen, Y.; Blau, W. J. *J. Mater. Chem.* **2009**, *19*, 7425–7443.
(13) Wang, Q.; Qin, Y.; Zhu, Y.; Huang, X.; Tian, Y.; Zhang, P.; Guo, Z.; Wang, Y. *Chem. Phys. Lett.* **2008**, *457*, 159–162.
(14) Zhang, L.; Thomas, J.; Allen, S. D.; Wang, Y. X. *Opt. Eng.* **2010**, *49*, 0638011–0638016.
(15) Qiu, X. Q.; Wu, H. X.; Tong, R.; Qian, S. X.; Lin, Y. H.; Cai, R. F. *Chin. Phys. Lett.* **2008**, *25*, 536–539.
(16) Chen, P.; Wu, X.; Sun, X.; Lin, J.; Ji, W.; Tan, K. L. *Phys. Rev. Lett.* **1999**, *82*, 2548–2551.
(17) Chin, K. C.; Gohel, A.; Elim, H. I.; Chen, W.; Ji, W.; Chong, G. L.; Sow, C. H.; Wee, A. T. S. *J. Mater. Res.* **2006**, *21*, 2758–2766.
(18) Jin, Z.; Sun, X.; Xu, G.; Goh, S. H.; Ji, W. *Chem. Phys. Lett.* **2000**, *318*, 505–551.
(19) Shoji, S.; Suzuki, H.; Zaccaria, R. P.; Sekkat, Z.; Kawata, S. *Phys. Rev. B: Condens. Matter Mater. Phys.* **2008**, *77*, 1534071–1534074.
(20) Byeong, G. K.; Young, J. L.; Jeong, K.; Lee, K.; Young, H. L.; Seung, H. L. *Nanotechnology* **2010**, *21*, 405202–405206.
(21) Bubke, K.; Gnewuch, H.; Hempstead, M.; Hammer, J.; Green, M. L. H. *Appl. Phys. Lett.* **1997**, *71*, 1906–1908.
(22) Li, D.; Xia, Y. *Adv. Mater.* **2004**, *16*, 1151–1170.
(23) Formhals, A. U.S. Patent 1 975 504, 1934.
(24) Reneker, D. H.; Chun, I. *Nanotechnology* **1996**, *7*, 216–223.
(25) Reneker, D. H.; Yarin, A. L.; Fong, H.; Koombhongse, S. *J. Appl. Phys.* **2000**, *87*, 4531–4547.
(26) Theron, A.; Zussman, E.; Yarin, A. L. *Nanotechnology* **2001**, *12* 384–390.
(27) Zussman, E.; Theron, A.; Yarin, A. L. *Appl. Phys. Lett.* **2003**, *82* 973–975.
(28) Li, D.; Ouyang, G.; McCann, J. T.; Xia, Y. *Nano Lett.* **2005**, *5* 913–916.
(29) Kim, G.; Kim, W. *Appl. Phys. Lett.* **2006**, *88*, 233101–2331013.
(30) Yang, D.; Lu, B.; Zhao, Y.; Jiang, X. *Adv. Mater.* **2007**, *19* 3702–3706.
(31) Yang, D.; Zhang, J.; Zhang, J.; Nie, J. *J. Appl. Polym. Sci.* **2008**, *110*, 3368–3372.
(32) Teo, W. E.; Ramakrishna, S. *Nanotechnology* **2006**, *17*, 89–106.
(33) Dror, Y.; Salalha, W.; Khalfin, R. L.; Cohen, Y.; Yarin, A. L.; Zussman, E. *Langmuir* **2003**, *19*, 7012–7020.
(34) Ko, F.; Gogotsi, Y.; Ali, A.; Naguib, N.; Ye, H.; Yang, G. L.; Li, C.; Willis, P. *Adv. Mater.* **2003**, *15*, 1161–1165.
(35) Salalha, W.; Dror, Y.; Khalfin, R. L.; Cohen, Y.; Yarin, A. L.; Zussman, E. *Langmuir* **2004**, *20*, 9852–9855.
(36) Liu, L-.; Tasis, D.; Prato, M.; Wagner, H. *Adv. Mater.* **2007**, *19* 1228–1233.
(37) Sundaray, B.; Jagadeesh, B. V.; Subramanian, V.; Natarajan, T. S. *J. Eng. Fiber. Fabr.* **2008**, *3*, 39–45.
(38) Liu, J.; Liu, T.; Kumar, S. *Polymer* **2005**, *46*, 3419–3424.
(39) He, J.; Wan, Y.; Yu, J. *Fiber. Polym.* **2008**, *9*, 140–142.
(40) Gupta, P.; Elkins, C.; Long, T. E.; Wilkes, G. L. *Polymer* **2005**, *46*, 4799–4810.
(41) Baumgarten, P. K. *J. Colloid Interface Sci.* **1971**, *36*, 71–79.
(42) Jiang, K.; Li, Q.; Fan, S. *Nature* **2002**, *419*, 801–801.